

RESEARCH ARTICLE

Enhanced superconductivity in hole-doped Nb₂PdS₅

Qian Chen^{1,3}, Xiaohui Yang^{1,3}, Xiaojun Yang^{1,3}, Jian Chen^{1,3}, Chenyi Shen^{1,3},
Pan Zhang^{1,3}, Yupeng Li^{1,3}, Qian Tao^{1,2}, Zhu-An Xu^{1,2,3,†}

¹Department of Physics and State Key Laboratory of Silicon Materials, Zhejiang University, Hangzhou 310027, China

²Zhejiang California International NanoSystems Institute, Zhejiang University, Hangzhou 310058, China

³Collaborative Innovation Centre of Advanced Microstructures, Nanjing 210093, China

Corresponding author. E-mail: †zhuan@zju.edu.cn

Received August 16, 2016; accepted October 12, 2016

We synthesized a series of Nb₂Pd_{1-x}Ru_xS₅ polycrystalline samples by a solid-state reaction method and systematically investigated the Ru-doping effect on superconductivity by transport and magnetic measurements. It is found that superconductivity is enhanced with Ru doping and is quite robust upon disorder. Hall coefficient measurements indicate that the charge transport is dominated by hole-type charge carriers similar to the case of Ir doping, suggesting multi-band superconductivity. Upon Ru or Ir doping, H_{c2}/T_c exhibits a significant enhancement, exceeding the Pauli paramagnetic limit value by a factor of approximately 4. A comparison of T_c and the upper critical field (H_{c2}) amongst the different doping elements on Pd site, reveals a significant role of spin-orbit coupling.

Keywords superconductivity, hole-doping, upper critical field, spin-orbit coupling, phase diagram

PACS numbers 74.70.Dd, 74.62.Dh, 74.62.-c

1 Introduction

The transition metal-chalcogenide compounds T₂PdCh₅, where T = Nb or Ta and Ch = S or Se, are quasi-one-dimensional (Q1D) superconductors with a remarkably high upper critical field [1–4], which surpasses by far the expected Pauli limiting field ($H_{c2}^{Pauli} = 1.84T_c$) [5]. These compounds achieving superconducting temperatures up to 6 K are proposed to be multi-band superconductors [1, 3, 6, 7]. Band structure calculations [1, 2, 7] show that the Fermi surface of Nb₂PdS₅ is composed of multiple sheets, i.e., two-dimensional sheets with hole character and Q1D sheets with both electron and hole character, and this system may be in proximity to a magnetically- or charge density wave- (CDW-) ordered state, owing to the nesting properties of those Q1D Fermi surface sheets. The increase in the *d* electron population on the Pd site is expected to flatten the Q1D Fermi surface sheets; thus, it may enhance the nesting properties and an unconventional superconducting pairing scenario is suggested [1, 7]. It is shown that partial substitution of Pd by Ni [8] or Ir [9] leads to slightly enhanced T_c , but superconductivity is suppressed in the cases of Pt-

for-Pd doping [8] or Ag-for-Pd doping [9], and Se-for-S doping [10]. However, the feature of large H_{c2} relative to T_c is found to be robust against these substitutions, providing strong experimental evidence of unconventional superconductivity in this system.

As is often the case, high superconducting critical field can be attributed to the multi-band effect [11], strong-coupling [12], spin-triplet pairing [13], or strong spin-orbit coupling (SOC) [14]. A study on the effect of selenium doping on Nb₂PdS₅ rules out the strong-coupling as well as spin-triplet pairing as the origin of the exotic superconductivity [10]. In contrast, it is suggested that the large H_{c2} can be attributed to the strong SOC associated with the heavy Pd element [4, 8, 12, 14]. Moreover, electronic structure calculations for Ta₂PdS₅ show that the large H_{c2} is a result of a combination of strong coupling and multi-band effects in the extreme dirty limit [7]. These experimental and theoretical studies have verified the importance of the presence of Pd irons with a large *Z* number to the unconventional properties, where *Z* is the atomic mass number. Recently, it has been reported that the charge carrier density (or band filling), which can be modulated by hole(electron)-type doping, could be a crucial factor for tuning superconductivity in this system [9]. So far, the origin of the large H_{c2} and exotic superconductivity in T₂PdCh₅ has not been un-

*arXiv: 1611.03724v1.

derstood.

In this paper, we report on a detailed investigation of the hole-type Ru doping effect on superconductivity and compare with the case of similar Ir doping. Both Ru and Ir doping on Pd site can be considered as a hole-type doping, but less heavy Ru should have a weaker SOC compared with Ir or Pt doping; thus, it may help with distinguishing the different effects of charge carrier density and SOC upon superconductivity. We make a comparison of the cases of Ir, Ag, Ni, and Pt doping and it turns out that T_c and H_{c2} can be slightly enhanced by hole-type doping such as Ru or Ir doping, but that Ir doping has a more significant effect owing to its stronger SOC. Our work implies that there could be a close relationship between the extremely large H_{c2} and SOC in this Q1D superconducting system.

2 Experimental details

We synthesized a series of $\text{Nb}_2\text{Pd}_{1-x}\text{Ru}_x\text{S}_5$ ($x = 0-1$) and $\text{Nb}_2\text{Pd}_{1-x}\text{Ir}_x\text{S}_5$ ($x = 0.1, 0.2, 0.4$) polycrystalline samples by the usual solid-state reaction method. More details can be found in our previous report [9]. Nb, Pd, Ir or Ru, and S of high purity (99.9%) were used as the starting materials. Energy-dispersive X-ray (EDX) spectroscopy analysis shows the presence of Pd-site deficiencies in this system, which are found to be about 0.25, similar to our previous report. The actual Ru composition of the obtained samples is in proportion to the nominal stoichiometric composition, and 70%–80% of the corresponding nominal Ru element is doped into the grains, as determined by the EDX analysis. Powder X-ray diffraction (XRD) measurements were performed at room temperature on a PANalytical X-ray diffractometer with Cu $K\alpha$ radiation and the lattice constants were

determined using the program X'Pert HighScore. The temperature dependence of magnetization was measured on a Quantum Design magnetic property measurement system (MPMS-5). The electrical resistivity and Hall coefficient (R_H) measurements were carried out in a physical property measurement system (PPMS-9) by a standard six-terminal method.

3 Results and discussion

Figure 1 shows XRD patterns of $\text{Nb}_2\text{Pd}_{1-x}\text{Ru}_x\text{S}_5$ ($x = 0-1$). The main peaks are well indexed based on a monoclinic cell with the space group C2/m, indicating the samples are almost single phase. Only a few minor impurity peaks marked by the asterisks are observed, which are unknown yet. The lattice parameters as a function of nominal x are presented in the right panel. Both a and b remain almost constant, while the c -axis shrinks significantly with increasing Ru doping. This result is consistent with the smaller ion radius of Ru compared with that of Pd. The structural characterization of Ir-doped $\text{Nb}_2\text{Pd}_{1-x}\text{Ir}_x\text{S}_5$ samples can be found in the previous report [9].

The temperature-dependent resistivity shown in Fig. 2 for all studied Ru-doped samples is normalized, whereby each value is divided by its individual absolute value at room temperature ($\rho_{300\text{K}}$). The resistivity at $T = 300\text{K}$ ranges from $1.55\text{ m}\Omega\cdot\text{cm}$ to $4.6\text{ m}\Omega\cdot\text{cm}$. For the parent compound Nb_2PdS_5 , the resistivity shows a metallic behavior upon decreasing temperature and then becomes superconducting below $T_c \sim 6\text{ K}$, consistent with previous reports [1, 9]. Upon doping with Ru, a small upturn shows up at a low temperature, which can be interpreted as the result of Anderson localization [4] or the grain boundary effect [15]. In the scenario of disorder-induced

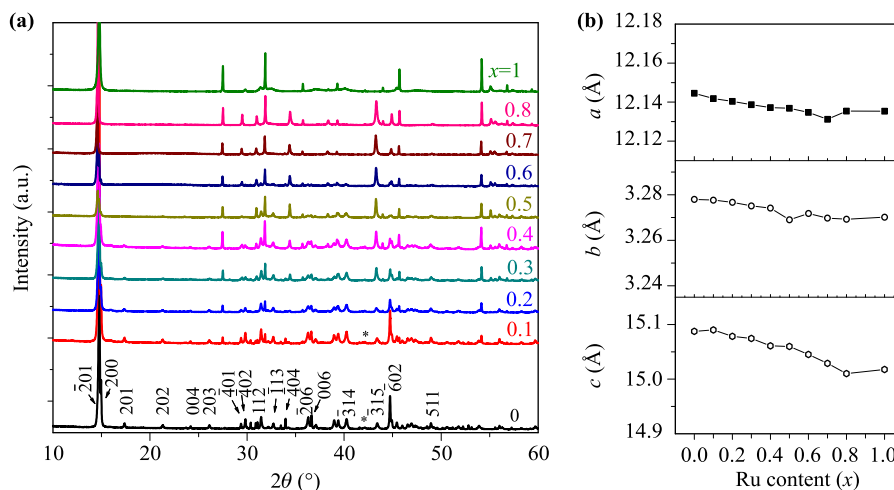


Fig. 1 (a) Room temperature powder X-ray diffraction patterns for the $\text{Nb}_2\text{Pd}_{1-x}\text{Ru}_x\text{S}_5$ samples with $x = 0-1$. (b) Variations of lattice constants as a function of nominal doping content x .

localization, a more profound resistivity upturn would be observed with the increase of doping. An expanded plot of the low-temperature regime below 10 K is presented in the lower inset of Fig. 2. Remarkably, the increase in Ru doping enhances superconductivity and T_c^{mid} reaches 6.9 K at $x = 0.2$, and then superconductivity is suppressed with further doping. In addition, we confirmed the bulk nature of superconductivity by the magnetic susceptibility measurements for all samples. The data for three samples ($x = 0, 0.2$, and 0.3) are presented in the upper right inset of Fig. 2. Strong diamagnetic signals were observed, and meanwhile the onset temperature of magnetic transitions obviously varies with the Ru content, which is consistent with the resistivity measurements.

In order to get an insight into the evolution of transport properties, the temperature dependence of the Hall coefficient at various doping levels was measured. As shown in Fig. 3, R_H is positive for the doped samples, indicating hole-type dominant charge carriers, as opposed to the n -type charge carriers in the parent compound. This confirms that Ru doping induces the holes into the system. It is noted that for the $x = 0.2$ sample, while R_H is negative at room temperature, it becomes positive and strongly T dependent below 200 K. In a scenario in which the Fermi surface contains both electron and hole pockets, the sign change of R_H as a function of temperature allows us to suggest that hole carriers dominate the transport properties at low temperature, owing to the different temperature dependence of mobility for different types of charge carriers, or possible reconstruction of the Fermi surface as reported in the

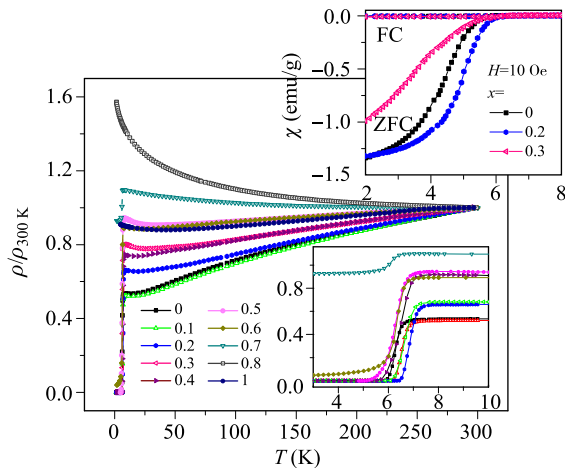


Fig. 2 Temperature dependence of the electrical resistivity of $\text{Nb}_2\text{Pd}_{1-x}\text{Ru}_x\text{S}_5$ normalized to $\rho_{300\text{K}}$. The lower inset shows the expanded view of resistivity versus T around the superconducting transition temperatures. The upper inset depicts temperature dependence of magnetic susceptibility under zero-field cooling (ZFC) and field cooling (FC) for $\text{Nb}_2\text{Pd}_{1-x}\text{Ru}_x\text{S}_5$ ($x = 0, 0.2$, and 0.3), respectively.

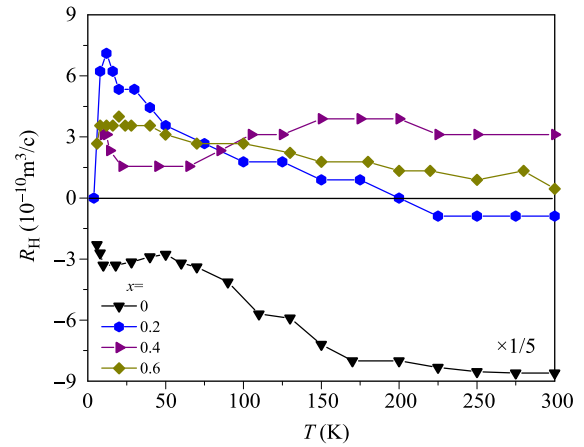


Fig. 3 Temperature dependence of the Hall coefficient for the four superconducting samples ($x = 0, 0.2, 0.4$, and 0.6). The data for undoped sample have been divided by 5 for clarity.

cuprates [16]. As for the undoped sample, whereas above 200 K, R_H is relatively insensitive to temperature, it monotonically increases with decreasing T . These data may provide evidence for the possible multi-band superconductivity. For conventional one-band metals, in contrast, weak temperature dependence of normal state R_H is usually observed. Beyond these considerations, it is known that in the transition metal dichalcogenides, the change in electronic structure due to magnetic ordering or CDW transition could lead as well to a sign change of the Hall coefficient [17]. Though the Nb_2PdS_5 system is predicted to be in proximity to a magnetic order or CDW state, there is no experimental evidence of this to date.

According to our previous work [9], partial substitution of Pd by Ir, which is also considered as hole-type doping, could obviously increase T_c for low Ir content, while Ag doping, which is regarded as electron-type doping, destroys superconductivity quickly. It is interesting to compare the effects of Ru doping with Ir doping, as both are regarded as hole-type dopants. Since the strength of SOC is proportional to Z^4 , Ru doping should hardly change the SOC associated with the Pd site, while Ir or Pt (Ni) doping could increase (decrease) the SOC in the system [8, 14]. Therefore, we may distinguish the effect of SOC from charge carrier density through comparing the effect of Ru doping with that of Ir doping.

Based on the resistivity measurements, a phase diagram of T_c vs. doping level for the $\text{Nb}_2\text{Pd}_{1-x}\text{Ru}_x\text{S}_5$ series is constructed as shown in Fig. 4. The data of Ir, Ag, Pt, and Ni doping (Refs. [8] and [9]) are also plotted for comparison. Ru and Ir doping are indicated by hollow symbols standing for hole doping; Ag doping is indicated by solid characters. It can be found that supercon-

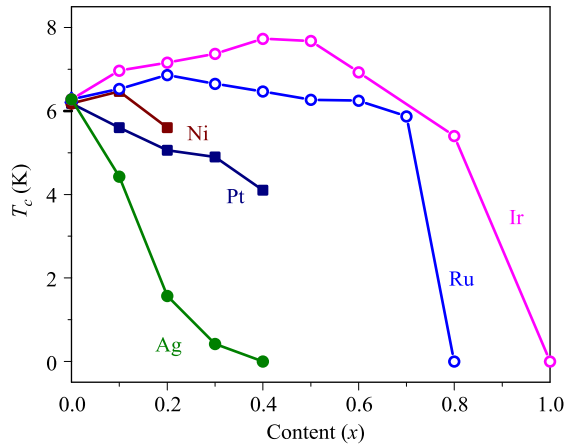


Fig. 4 T_c as a function of doping level x for $\text{Nb}_2\text{Pd}_{1-x}\text{R}_x\text{S}_5$, extracted from the resistivity where $\rho(T)$ drops to 50% of the normal state value. The variations of T_c of $\text{Nb}_2\text{Pd}_{1-x}\text{R}_x\text{S}_5$, $R = \text{Ir}, \text{Ag}, \text{Ni}$ or Pt , is also plotted for comparison. The data for Ni and Pt doping are taken from Ref. [8]. The data for Ir and Ag doping are from our previous work [9]. The hollow symbols stand for hole doping, Ru and Ir, distinct from other dopings which are in solid symbols.

ductivity is enhanced with a maximum T_c^{mid} of 6.86 K by Ru ($x = 0.2$) doping, and 7.73 K by Ir ($x = 0.4$) doping. Both Ru and Ir doping are expected to increase the hole-type carrier density, which may drive the system far away from the magnetic order or a possible CDW order and thus favor superconductivity, while the electron-type doping (i.e., Ag doping) has an opposite effect. In this scenario, we could understand why T_c initially increases for both Ru doping and Ir doping. However,

the maximum T_c is even higher and the superconducting range (up to x of 0.8) is wider for the Ir doping case. We propose that the enhanced SOC strength owing to heavier Ir may account for this difference. This result implies that not only the charge carrier density but also SOC could play an important role in controlling superconductivity of Nb_2PdS_5 . As in the case of Pt or Ni doping, superconductivity can be easily suppressed, which may be ascribed to the positive internal pressure effect corresponding to the shrinking of the c -axis by the isovalent substitution of Pd, in spite of the enhanced SOC in the Pt case. It should also be noted that superconductivity can survive up to very high doping level in the cases of Ru or Ir doping despite the disorder, which demonstrates that T_c is quite robust in the hole-type doping, as compared with the iron-based superconductors $\text{LaFe}_{1-x}\text{Co}_x\text{AsO}$ [18] and $\text{BaFe}_{2-x}\text{Ni}_x\text{As}_2$ [19]. Careful studies on the single-crystalline $\text{Nb}_2\text{Pd}_x\text{S}_{5-\delta}$ revealed that superconductivity occurs in a wide range of Pd ($0.6 < x < 1$) and S ($0 < \delta < 0.61$) contents [20], suggesting again that superconductivity in this system is very robust.

Since a previous study proposed that changes in the SOC may affect the large upper critical field (H_{c2}) [8], it is very helpful to compare the ratio of H_{c2} to T_c for different doping cases. We measured the temperature-dependent resistivity for applied magnetic fields up to 15 T to get the upper critical field data H_{c2} for the two series of samples $\text{Nb}_2\text{Pd}_{1-x}\text{Ru}_x\text{S}_5$ and $\text{Nb}_2\text{Pd}_{1-x}\text{Ir}_x\text{S}_5$, as shown in Fig. 5. The resultant H_{c2} data are summarized in Figs. 5(a) and (b) together with the theoretical Ginzberg–Landau (GL) fits (solid line) [14]. The H_{c2} values were deduced from the fields at which $\rho(T)$ drops

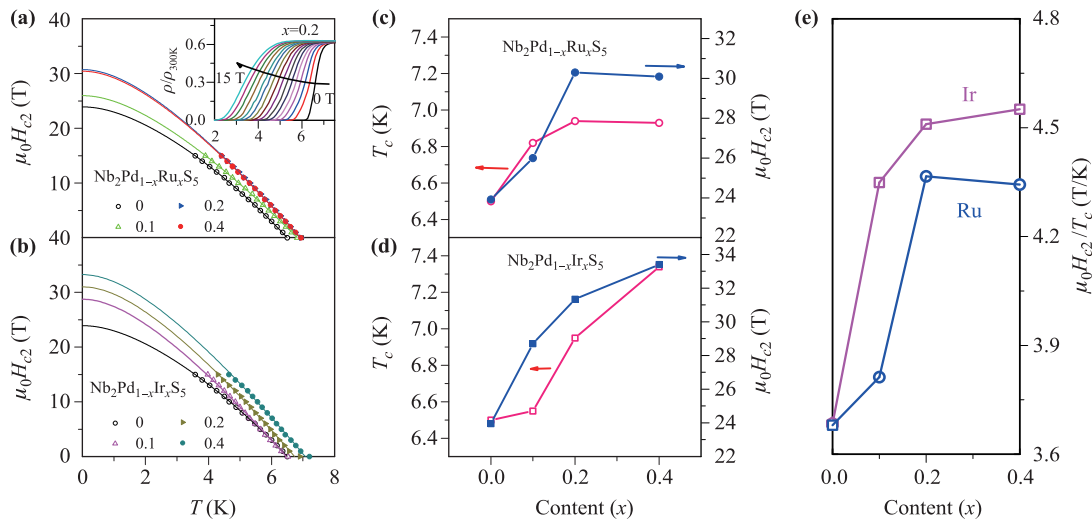


Fig. 5 (a, b) Comparison of the upper critical field data H_{c2} for $\text{Nb}_2\text{Pd}_{1-x}\text{Ru}_x\text{S}_5$ and $\text{Nb}_2\text{Pd}_{1-x}\text{Ir}_x\text{S}_5$. Inset: Resistivity as a function of temperature under several magnetic field (0–15 T). (c, d) The doping dependence of extrapolated $H_{c2}(0)$ and T_c values. (e) Variations in H_{c2}/T_c values with the doping content.

to 90% of the normal state value and the data can be well described by the GL equation. In Figs. 5(c) and (d), the variations in extrapolated $H_{c2}(0)$ values with the doping content are displayed. For the $\text{Nb}_2\text{Pd}_{1-x}\text{Ru}_x\text{S}_5$ samples, $H_{c2}(0)$ is initially enhanced and then goes down with the Ru substitution. In the case of Ir doping, $H_{c2}(0)$ is revealed to monotonically increase with increasing doping. In addition to the $H_{c2}(0)$ data, T_c is shown for comparison. Roughly speaking, the tendency of $H_{c2}(0)$ is in good agreement with T_c . Compared with the calculated $H_{c2}(0)$ data using the single-band Wethamer–Helfand–Hohenberg (WHH) model $H_{c2}(0) = -0.69T_c (dH_{c2}/dT)_{T_c}$, the difference in the $H_{c2}(0)$ values is below 5%. In Fig. 5(e), a phase diagram for H_{c2}/T_c with respect to variation of doping content is presented. Upon increasing the doping level, H_{c2}/T_c exhibits a significant enhancement in this system, exceeding the Pauli paramagnetic limit value ($1.84T_c$) by a factor of 3.8 to 4.6. This behavior is in support of the fact that hole-type doping benefits superconductivity and thus gives rise to larger upper critical fields. Moreover, a greater enhancement of H_{c2}/T_c in $\text{Nb}_2\text{Pd}_{1-x}\text{Ir}_x\text{S}_5$ series than $\text{Nb}_2\text{Pd}_{1-x}\text{Ru}_x\text{S}_5$ is observed, which may originate from an additional SOC effect on the one-dimensional Pd chains by Ir doping, in the framework of the scenario in which high superconducting upper critical field may arise from strong SOC, as evidenced from the opposite H_{c2}/T_c tendency in the Pt and Ni doping cases, reported by Zhou *et al.* [8] These findings again suggest that charge carrier as well as the large SOC in this system have significant effects on superconductivity. It is noted that H_{c2}/T_c at $x = 0.4$ for Ru doping goes down slightly. The suppression could be ascribed to impurity effects at a high doping level.

4 Conclusion

In conclusion, we compared the effects of Ru and Ir doping on superconductivity in the Nb_2PdS_5 system. The enhancement in both T_c and H_{c2} is observed upon partial Ru (or Ir) substitution and the hole-type dominant charge transport property are confirmed by Hall coefficient measurements. However, the increases in T_c and the ratio H_{c2}/T_c is more significant in the Ir doping case than in the Ru doping case. Given that SOC in the system could be hardly changed by Ru doping, but enhanced by Ir doping, the comparison of the two doping cases suggests that there is a correlation between the SOC and the enhanced H_{c2}/T_c ratio. Our work reveals that the exotic superconductivity in this system could be related to the strong SOC on the Pd site.

Acknowledgements The authors would like to thank Guanghan Cao for helpful discussions. This work was supported

by the Ministry of Science and Technology of China (Grant Nos. 2014CB921203 and 2016YFA0300402), the National Natural Science Foundation of China (Contract Nos. U1332209 and 11190023), the Ministry of Education of China (Contract No. 2015KF07), and the Fundamental Research Funds for the Central Universities of China.

References

1. Q. Zhang, G. Li, D. Rhodes, A. Kiswandhi, T. Besara, B. Zeng, J. Sun, T. Siegrist, M. D. Johannes, and L. Balicas, Superconductivity with extremely large upper critical fields in $\text{Nb}_2\text{Pd}_{0.81}\text{S}_5$, *Sci. Rep.* 3, 1446 (2013)
2. S. Khim, B. Lee, K. Y. Choi, B. G. Jeon, D. H. Jang, D. Patil, S. Patil, R. Kim, E. S. Choi, S. Lee, J. Yu, and K. H. Kim, Enhanced upper critical fields in a new quasi-one-dimensional superconductor $\text{Nb}_2\text{Pd}_x\text{Se}_5$, *New J. Phys.* 15(12), 123031 (2013)
3. J. Zhang, J. K. Dong, Y. Xu, J. Pan, L. P. He, L. J. Zhang, and S. Y. Li, Superconductivity at 2.5 K in the new transition-metal chalcogenide $\text{Ta}_2\text{Pd}_x\text{Se}_5$, *Supercond. Sci. Technol.* 28(11), 115015 (2015)
4. Y. Lu, T. Takayama, A. F. Bangura, Y. Katsura, D. Hashizume, and H. Takagi, Superconductivity at 6 K and the violation of Pauli limit in $\text{Ta}_2\text{Pd}_x\text{S}_5$, *J. Phys. Soc. Jpn.* 83(2), 023702 (2014)
5. A. M. Clogston, Upper limit for the critical field in hard superconductors, *Phys. Rev. Lett.* 9(6), 266 (1962)
6. Q. R. Zhang, D. Rhodes, B. Zeng, T. Besara, T. Siegrist, M. D. Johannes, and L. Balicas, Anomalous metallic state and anisotropic multiband superconductivity in $\text{Nb}_3\text{Pd}_{0.7}\text{Se}_7$, *Phys. Rev. B* 88(2), 024508 (2013)
7. D. J. Singh, Electronic structure and upper critical field of superconducting $\text{Ta}_2\text{Pd}_x\text{S}_5$, *Phys. Rev. B* 88(17), 174508 (2013)
8. N. Zhou, X. Xu, J. R. Wang, J. H. Yang, Y. K. Li, Y. Guo, W. Z. Yang, C. Q. Niu, B. Chen, C. Cao, and J. Dai, Controllable spin-orbit coupling and its influence on the upper critical field in the chemically doped quasi-one-dimensional Nb_2PdS_5 superconductor, *Phys. Rev. B* 90(9), 094520 (2014)
9. C. Y. Shen, B. Q. Si, H. Bai, X. J. Yang, Q. Tao, G. H. Cao, and Z. A. Xu, Pd site doping effect on superconductivity in $\text{Nb}_2\text{Pd}_{0.81}\text{S}_5$, *Europhys. Lett.* 113(3), 37006 (2016)
10. C. Q. Niu, J. H. Yang, Y. K. Li, B. Chen, N. Zhou, J. Chen, L. L. Jiang, B. Chen, X. X. Yang, C. Cao, J. Dai, and X. Xu, Effect of selenium doping on the superconductivity of $\text{Nb}_2\text{Pd}(\text{S}_{1-x}\text{Se}_x)_5$, *Phys. Rev. B* 88(10), 104507 (2013)
11. A. Gurevich, Enhancement of the upper critical field by nonmagnetic impurities in dirty two-gap superconductors, *Phys. Rev. B* 67(18), 184515 (2003)
12. J. P. Carbotte, Properties of boson-exchange superconductors, *Rev. Mod. Phys.* 62(4), 1027 (1990)

13. I. J. Lee, P. M. Chaikin, and M. J. Naughton, Exceeding the Pauli paramagnetic limit in the critical field of $(\text{TMTSF})_2\text{PF}_6$, *Phys. Rev. B* 62(22), R14669 (2000)
14. N. R. Werthamer, E. Helfand, and P. C. Hohenberg, Temperature and purity dependence of the superconducting critical field, H_{c2} (III): Electron spin and spin-orbit effects, *Phys. Rev.* 147(1), 295 (1966)
15. A. Carrington and J. R. Cooper, Influence of grain-boundary scattering on the transport properties of a high- T_c oxide superconductor, *Physica C* 219(1-2), 119 (1994)
16. D. LeBoeuf, N. Doiron-Leyraud, J. Levallois, R. Daou, J. B. Bonnemaïson, N. E. Hussey, L. Balicas, B. J. Ramshaw, R. Liang, D. A. Bonn, W. N. Hardy, S. Adachi, C. Proust, and L. Taillefer, Electron pockets in the Fermi surface of hole-doped high- T_c superconductors, *Nature* 450(7169), 533 (2007)
17. H. N. S. Lee, M. Garcia, H. McKinzie, and A. Wold, The low-temperature electrical and magnetic properties of TaSe_2 and NbSe_2 , *J. Solid State Chem.* 1(2), 190 (1970)
18. C. Wang, Y. K. Li, Z. W. Zhu, S. Jiang, X. Lin, Y. K. Luo, S. Chi, L. J. Li, Z. Ren, M. He, H. Chen, Y. T. Wang, Q. Tao, G. H. Cao, and Z. A. Xu, Effects of cobalt doping and phase diagrams of $\text{LFe}_{1-x}\text{Co}_x\text{AsO}$ ($L = \text{La}$ and Sm), *Phys. Rev. B* 79(5), 054521 (2009)
19. L. J. Li, Y. K. Luo, Q. B. Wang, H. Chen, Z. Ren, Q. Tao, Y. K. Li, X. Lin, M. He, Z. W. Zhu, G. H. Cao, and Z. A. Xu, Superconductivity induced by Ni doping in BaFe_2As_2 single crystals, *New J. Phys.* 11(2), 025008 (2009)
20. H. Yu, M. Zuo, L. Zhang, S. Tan, C. Zhang, and Y. Zhang, Superconducting fiber with transition temperature up to 7.43 K in $\text{Nb}_2\text{Pd}_{1-x}\text{S}_5$ ($0.6 < x < 1$), *J. Am. Chem. Soc.* 135(35), 12987 (2013)